Preprints of the 18th IFAC World Congress
Milano (Italy) August 28 - September 2, 2011

Gain-Scheduled Yaw Control for Aircraft Ground Taxiing

D. Lemay * **Y. Chamaillard** ** **M. Basset** *** **J.P. Garcia** *

* *Messier-Bugatti, Safran Group, ZA Louis Bréguet, BP 40, 78141 Vélizy Cedex, France (e-mail: david.lemay@messier-bugatti.com)*
** *PRISME, Université d'Orléans, 8 rue Léonard de Vinci, 45072 Orléans Cedex 2, France (e-mail: yann.chamaillard@univ-orleans.fr)*
*** *MIPS, Université de Haute Alsace, 12 rue des Frères Lumière, 68093 Mulhouse Cedex, France, (e-mail: michel.basset@uha.fr)*

Abstract: a gain scheduled yaw controller is proposed to control low speed rolling and manoeuvring of an aircraft on ground. This method is based on local linearisation of a non-linear model and the synthesis of a family of local controllers. A parallel feedforward action is added to achieve the setpoint tracking and let the feedback controller perform the regulation task. Simulation results show attractive and robust performances regard to the adopted control method.

Keywords: Aircraft control ; Gain-Scheduling ; Feedforward ; Model reference control

1. INTRODUCTION

Currently, the on-ground motion of the aircraft is manually driven by coordinating actions on each individual system. The pilot has six controls: the thrust of the left and right engines, the rudder deflection, the left and right brake pressure, and the nose wheel steering angle. This piloting task is quite demanding since those systems have heterogeneous and highly non-linear dynamics. Moreover, the aircraft behaviour dramatically varies with external conditions (runway contamination, wind, *etc.*). Those inconveniences divert the pilot from its prime task: guiding and maintaining the aircraft in a safe situation with regard to infrastructure and neighbour vehicles (Fig. 1). Then, a need arises for a piloting aid in order to let the

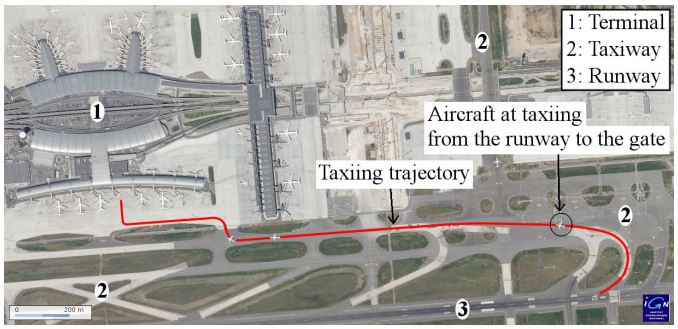

(C) GEOPORTAIL

Fig. 1. Aircraft at taxiing

pilot concentrating on the guiding and safety questions. Interactions between the pilot and the control system involve achieving a trajectory response compatible with human handling characteristics. In a farer term, a ground autopilot is foreseen – alike the flight one – to guide the aircraft across the taxiways. This automatic system would enable airlines to operate in conditions where the human pilot is unable, in poor visibility for instance. It would also improve the ground traffic capacity of airports by communicating with a traffic manager which would optimize the vehicle flow on the airport area (Villaume, 2002).

In addition, air transportation research has focused on overall reduction of pollutants and especially on minimisation of ground noise and exhaust gas emissions. One topic considers the benefits of driving the aircraft by means of electromechanical actuators located in the main landing gears (MLG) instead of main engines (Teo et al., 2008). This new propulsion system has the advantage of being silent and offers a much better efficiency than traditional jet engines. Work is ongoing to install such systems on each wheel of the main landing gears. Thereby, the rolling dynamics is greatly affected since the new driving system exhibits lower torque capacity but faster dynamics than the older. Differential driving and braking can now support the nose landing gear (NLG) steering system to control the lateral motion of the vehicle. They have complementary properties, the steering system provides a large yaw moment but is fairly slow, whereas differential driving has a limited moment capacity but exhibits fast dynamics (Fig. 2). This paper presents a method for controlling the yaw dynamics of an aircraft. First the model used for the synthesis is introduced in section 2. Section 3 exhibits the control design and its robustness is analysed in section 4. Finally, some simulation results, performed on a reference model, are shown in section 5 and section 6 gives a short conclusion.

LIST OF SYMBOLS

$\alpha_{N(M)}$	Slip angle of NLG (MLG)
$C_{N(M)}$	Cornering stiffness of NLG (MLG)
$Fy_{N(M)}$	Cornering force at NLG (MLG) contact point
Iz	Yaw moment of inertia of the vehicle

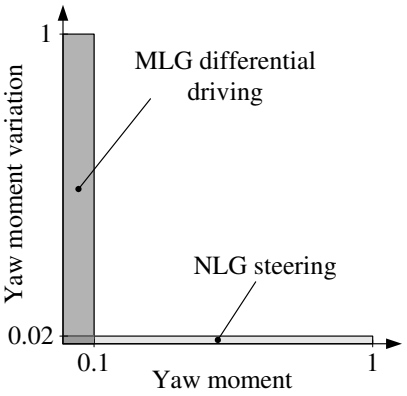

Fig. 2. Envelope of both static and dynamic actuator capacity at providing yaw moment

$Lx_{N(M)}$	Longitudinal distance between CG and NLG (MLG)
m	Mass of the vehicle
Mz	Global yaw moment: $Mz = Mz_N + Mz_{Md}$
Mz_N	Yaw moment provided by NLG
Mz_{Md}	Yaw moment provided by MLG differential driving
r	Yaw rate of the vehicle (state variable)
θ_N	Steering angle of NLG
$V_{N(M)}$	Velocity vector at NLG (MLG) contact point
V_{CG}	Velocity vector at CG
Vx	Longitudinal velocity at CG
Vy	Lateral velocity at CG (state variable)

2. SYSTEM MODELLING

A grounded short haul aircraft is a tricycle vehicle with symmetric MLG and a unique steerable NLG (Fig. 3). MLG wheels are both driven and braked and NLG ones are free rolling. The taxiing phase is performed at fairly low speed therefore roll dynamics appears negligeable. A simplified control-oriented model will be developped in this section. This simplified model only considers the lateral dynamics of the vehicle.

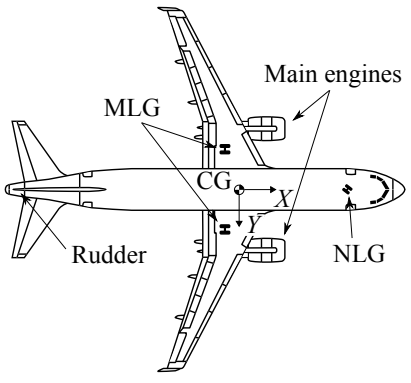

Fig. 3. Schematic short haul aircraft viewed from top

2.1 Lateral vehicle model

The rolling vehicle can be described by the well known planar *bicycle model* (Fig. 4). All wheels located on a same axis are considered as a unique wheel lying on the median plane of the vehicle. The rolling system is assumed to be parallel to the ground and neither roll, nor pitch, nor vertical dynamics are considered. Aerodynamic effects are

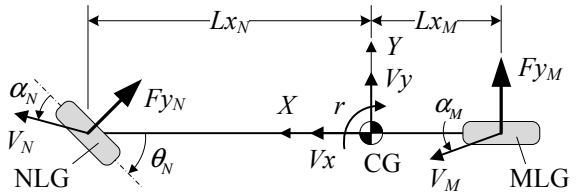

Fig. 4. Bicycle model

assumed negligible since low speed rolling is considered here, thus only ground contact forces are modelled. The friction contact force acting at each point is denoted Fy_N and Fy_M for the NLG (resp. MLG). V_N, V_M and V_{CG} denote the velocity vector at the nose and main contact points and at the center of gravity of the vehicle (CG). The longitudinal distance between the CG and the contact points is denoted by Lx_N and Lx_M. θ_N represents the nose wheel steering angle. The lateral velocity Vy and the yaw rate r are chosen as state variables expressed at the CG. The longitudinal velocity Vx is considered as an input exogenous parameter known by measurement or estimation. The equations of lateral dynamics are given here below:

$$\begin{aligned} Iz \cdot \dot{r} &= Lx_N \cdot Fy_N \cdot \cos(\theta_N) - Lx_N \cdot Fy_M + Mz_{Md} \\ m \cdot (\dot{Vy} + Vx \cdot r) &= Fy_N \cdot \cos(\theta_N) + Fy_M \end{aligned} \quad (1)$$

Iz is the yaw moment of inertia, m is the mass of the vehicle and Mz_{Md} stands for the yaw moment produced by differential driving of the MLG.

2.2 Contact force model

In equation 1, the cornering forces (Fy_N,Fy_M) are assumed to be linear with the slip angle (α_N,α_M) and with the equivalent cornering stiffness (C_N,C_M). This is true while the slip angles remain in a bounded region around zero.

$$Fy_N = -C_N \cdot \alpha_N \,, \quad C_N > 0 \quad (2)$$

$$Fy_M = -C_M \cdot \alpha_M \,, \quad C_M > 0 \quad (3)$$

Given :

$$\tan(\alpha_N + \theta_N) = \frac{Vy + Lx_N \cdot r}{Vx} \quad (4)$$

$$\tan(\alpha_M) = \frac{Vy - Lx_M \cdot r}{Vx} \quad (5)$$

The vehicle lateral dynamics is highly non-linear because of its longitudinal velocity and slip angles dependency. Note that, even at low speed ($Vx \in [0; 10]$ m/s), the non-linearity with regard to velocity is important (Fig. 5). A widespread method is to linearise the slip angle expressions (4) and (5) for small slip quantities and small steering angle (Zheng and Anwar, 2009). The latter assumption cannot be made during low speed taxiing and manoeuvring where the steering angle reaches 75 deg. To cope with the dynamics dispersion, a linearisation was made over a discrete domain of both the longitudinal velocity Vx and the lateral equilibrium, instead of a single point close to zero.

2.3 Model linearisation

Noting $\Phi = (Vy_e; r_e; \theta_{Ne})^T$ an equilibrium point of the dynamical system (1). A change of control variable has been performed to use the NLG yaw moment Mz_N as command instead of the steering angle. The first order linearisation, at this point Φ, gives the local linear state space form:

$$\begin{bmatrix} \dot{\delta r} \\ \dot{\delta Vy} \end{bmatrix} = \begin{bmatrix} A_{11} & A_{12} \\ A_{21} & A_{22} \end{bmatrix} \begin{bmatrix} \delta r \\ \delta Vy \end{bmatrix} + \begin{bmatrix} 1 & 1 \\ B_2 & 0 \end{bmatrix} \begin{bmatrix} \delta Mz_N \\ Mz_{Md} \end{bmatrix} \quad (6)$$

with δr and δVy the new state variables representing the variation of the local system in the vicinity of the equilibrium point. δMz_N is the additional yaw moment produced by the NLG. The state matrix terms express as follow :

$$A_{11} = -\frac{1}{Iz \cdot Vx} \left(\frac{C_M \cdot {Lx_M}^2}{1 + {\Delta_M}^2} + \frac{C_N \cdot {Lx_N}^2 \cdot \cos(\theta_{Ne})}{1 + {\Delta_N}^2} \right)$$

$$A_{12} = \frac{1}{Iz \cdot Vx} \left(\frac{C_M \cdot Lx_M}{1 + {\Delta_M}^2} - \frac{C_N \cdot Lx_N \cdot \cos(\theta_{Ne})}{1 + {\Delta_N}^2} \right)$$

$$A_{21} = \frac{1}{m \cdot Vx} \left(\frac{C_M \cdot Lx_M}{1 + {\Delta_M}^2} - \frac{C_N \cdot Lx_N \cdot \cos(\theta_{Ne})}{1 + {\Delta_N}^2} \right) - Vx$$

$$A_{22} = \frac{1}{m \cdot Vx} \left(\frac{C_M}{1 + {\Delta_M}^2} - \frac{C_N \cdot \cos(\theta_{Ne})}{1 + {\Delta_N}^2} \right)$$

$$B_2 = \frac{Iz}{m \cdot Lx_N}$$

The terms Δ_N and Δ_M reflect the state matrix dependency on the operating point $(\Phi, Vx)^T$:

$$\Delta_N(\Phi, Vx) = \frac{Vy_e + Lx_N \cdot r_e}{Vx}$$

$$\Delta_M(\Phi, Vx) = \frac{Vy_e - Lx_M \cdot r_e}{Vx}$$

These terms tend to zero as the cornering slip of the wheels vanishes. Then the state matrix corresponds to the one obtained assuming small slip angle (Zheng and Anwar, 2009).

Remark 1. The linearised system (6) features a second order dynamics which turns out to be quite close to a first order system, because of one pole-zero compensation. Moreover, if the second input Mz_{Md} may improve the system performance in a MIMO control loop, it is powered by the differentiel driving. The system is already employed by the longitudinal task and has a very limited action on the yaw moment (fig. 2). That is why it not considered in the rest of the article and will be studied in a future work. Thereby, the SISO first order model will be used for synthesis in the following section.

Figure 5 depicts both the static gain G_{ol} and time constant τ_{ol} of the equivalent first order model. The time constant range is fairly large (1:10 ratio) and highly depends on the vehicle velocity. This characteristic will have a great impact on the controller design.

2.4 Model validation

This synthesis model (remark 1) is compared to a complete 3-dimensions model which counts 16 degrees of freedom

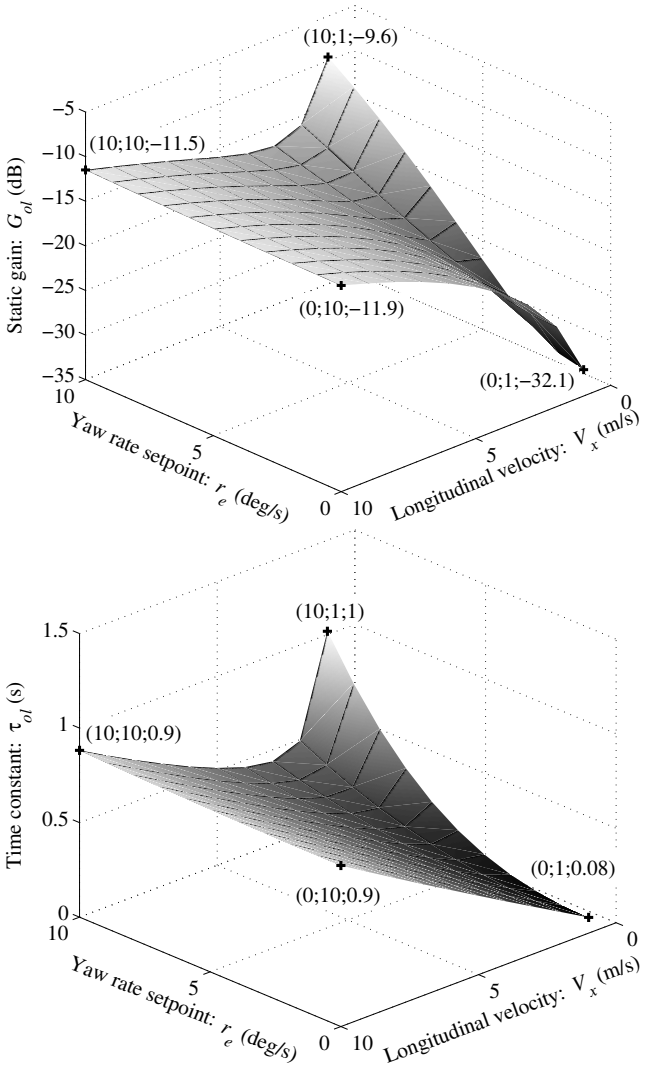

Fig. 5. Static gain & time constant of the equivalent 1st order model vs longitudinal velocity and yaw rate setpoint

(Slama, 2009) and more accurate tyre models (Albero, 2009). Three simulations were performed at distinctive setpoints. The figure 6 shows a good adequateness between each response. At low speed ($Vx = 1\,\mathrm{m/s}$) and high steering angle ($\theta_{Ne} = 50\,\mathrm{deg}$), the linearised model depicts a higher static gain than the reference one. Nevertheless, the dynamics seem to be fairly close to each other. This is the most important characteristic to match since any steady state error could be cancelled by an integral term in the controller. The model is aimed at synthesising a controller, not at performing feedforward control. At higher velocity and smaller steering angle, the synthesis model tightly fits the reference one. The dynamics difference in transient response comes from dynamics and slew rate limitation of the steering system which are not taken into account in the linearised model.

3. CONTROL STRUCTURE DESIGN

3.1 Control specifications

Though flight control has been studied for decades, aircraft rolling dynamics is a relatively new issue of interest.

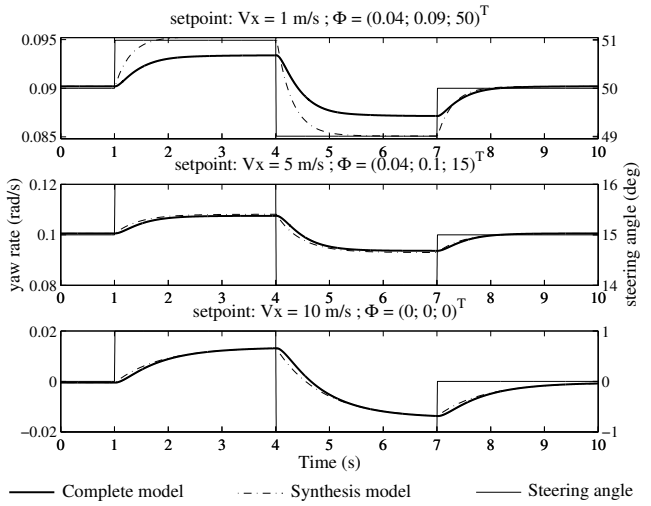

Fig. 6. Lane change manoeuvre of both the complete and linearised models at three setpoints (Yaw rate is labelled on left, steering angle is on right)

Ground interactions are highly non-linear and, above all, quite uncertain. (Duprez et al., 2004) proposed a yaw rate control by feedback linearisation with a particular logic to extend the method to vanishing velocity. (Roos and Biannic, 2006) adopted an LFT representation to design an adaptive anti-windup suitable to handle saturations of systems and tire adhesion. A prolific literature exists in the road vehicles domain where studies have widely focused on lateral control at relatively high speed (Zheng and Anwar, 2009). The robotic domain also counts tremendous papers dealing with mobile robot control (Mauder, 2008). However those works usually consider kinematic vehicle model or even ideal dynamic models with nonholonomic constrains (Pourboghrat and Karlsson, 2002). This hypothesis cannot be made for heavy vehicles such as planes rolling on various and potentially slippery surfaces.

The yaw control has to fit in a general control architecture suitable for interfacing with both a pilot and a future automatic guiding unit and with existing on-board systems (Jacquet, 2008). Then it must satisfy the requirements for automatic path tracking while being compatible with pilots feeling. The latter are familiar with a common vehicle handling and the assistance control has not to bother them. Hence the control method must ensure no steady state error and a settling time comparable to the natural response of the vehicle with no overshoot over the whole operating span. For testing purpose, the pilot shall still be able to manually steer the NLG while the aircraft is stationary. Moreover, to improve the aircraft manoeuvrability and to support the standard steering system in case of failure or lack of efficiency, differential driving is foreseen by means of the wheel actuators and brakes. The controller should cope with this additional yaw actuator in parallel to the NLG steering system.

All these considerations lead to implement a control method combining a feedforward action in parallel to an additive feedback non-linear controller. The feedforward term offers a similar control to the current open loop method and brings a naturally stable contribution. The feedback controller adds a local regulation action to ensure the cancellation of the steady state error.

3.2 Feedforward Command

A natural lateral vehicle handling is to control the direction of travel, *i.e.* the angle β_N between the longitudinal axis of the vehicle and the direction the pilot is pointing toward. On the other hand, a suitable reference variable for automatic control is the yaw rate of the vehicle. The two variables can easily be linked by an ideal kinematic model (Fig. 7) assuming no side slip of the wheels (7). This approximation remains reasonable while the aircraft operates in safe conditions. The kinematic model enables to command an open loop term θ_{ff} from the equality $\theta_{ff} = \beta_N$. Thereby, in manual control, the pilot commands

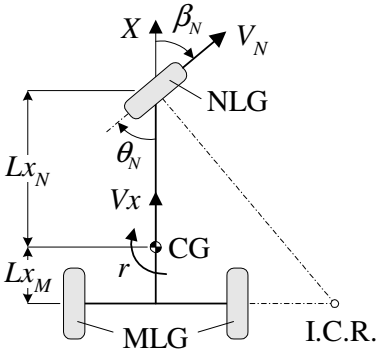

Fig. 7. Ideal kinematic model (I.C.R : Instantaneous Centre of Rotation)

the sight angle β_{Nc} whereas, in automatic piloting, the guiding unit sets the yaw rate demand r_c. The latter is converted into a feedforward command θ_{ff} by solving equation (7) for β_{Nc} and substituting θ_{ff} for β_{Nc}. Then a proper processing is made on the measured longitudinal velocity Vx_m to ensure no division by zero. This treatment must be robust to both measurement bias and noise amplitude. In fact, the limitation on Vx_m is part of the non-holonomic constrains of the rolling vehicle since it cannot rotate at a standstill. Therefore, the yaw task is itself not defined at this singular point.

$$r_c = \frac{Vx_m}{Lx_N + Lx_M} \cdot \tan(\beta_{Nc}) \tag{7}$$

This open loop command θ_{ff} acts as a tracking command and brings the vehicle yaw rate in the neighbourhood of the demand. This action has the benefit of being intrinsically stable. In parallel to the feedforward action, the pilot seat angle demand β_N is translated into a yaw rate remand r_c with the equation (7). Then, the controller can operate at the setpoint as a disturbance compensator to keep the measured yaw rate r_m equal to the demand r_c. Assuming the feedforward action steers the system close to the yaw rate demand, the equilibrium point can be worked out from the demand. This allows for adapting the controller to the current operating point.

3.3 Local controller design

The system (1) is assumed to be in the vicinity of an equilibrium point Φ. In order to ensure the steady state error cancellation, a PI-controller is proposed. The global yaw moment $Mz = \delta Mz_N + Mz_M$ is chosen as the controller output. This variable is independent from any

actuation system and can be delivered by either the steering system, a differential driving or a combination of both. Only the NLG steering is considered in this paper hence the equality $\delta Mz_N = Mz$ is assumed. The simplified first order model is considered (remark 1) and its time constant is denoted by τ_{ol}. Among the different methods of compensator synthesis, the time domain one is chosen here and the frequency analysis is performed in a validation process. The controller synthesis consists in finding both the proportional Kp and integral Ki gains to make the close loop system follow a reference first order model trajectory with time constant is τ_{cl}. Expressing the close loop transfer function H_{cl} gives:

$$H_{cl} = \frac{1 + Kp/Ki \cdot s}{1 + \tau_{ol} \cdot s} \frac{1}{\frac{1}{G_{ol} \cdot Ki} \cdot s + \frac{1+Kp/Ki \cdot s}{1+\tau_{ol} \cdot s}} \tag{8}$$

s is the Laplace variable. The pole compensation technique, equalizing $Kp/Ki = \tau_{ol}$, gives a first order transfer function which time constant can be chosen by a proper tuning of the Ki gain: $Ki = 1/(G_{ol} \cdot \tau_{cl})$. The steering system rate saturation dramatically limits the achievable dynamics. Thus, the close loop reference model is chosen to give no more than twice as fast a response as the open system ($\tau_{cl} = \tau_{ol}/2$). As simulation results will show up, this objective already makes the most of the steering system.
The linear PI-controller yields the required yaw moment δMz_N to cancel the yaw rate error $r_c - r_m$. The corrective NLG steering angle θ_{fb} is then worked out using the non-linear model of section 2.1:

$$\theta_{fb} = \frac{Iz}{C_N \cdot Lx_N \cdot \cos(\theta_N)} \cdot Mz_N \tag{9}$$

Either the measured steering angle or the speed vector orientation angle can be used for θ_N in equation (9). This term carries the non-linearity. It explicitly depends on the total steering angle, therefore it is valid over the whole operating range.

3.4 Gain Scheduling

The aforementioned local controller is to be extend to the whole operating range of the vehicle. The gain scheduling method may be one of the most popular approach of non-linear control. It has successfully been applied on a broad range of applications and a variety of methods have been proposed. One can refer to (Leithead, 1999) for an extended review of the literature. The classic approach is adopted here, *i.e.* a family of local controllers is synthesized at each equilibrium points and the non-linear controller is realized by linear interpolation of the gains (Rugh and Shamma, 2000). The span of the open loop dynamics (Fig. 5) is too large to achieve a unique close loop time response for all operating points. Indeed, it could be annoying for the pilot to loose the span of the lateral dynamics, especially the velocity dependence. That is why the close loop time response τ_{cl} is also scheduled with regard to the operating point in order to halve the open loop free settling time. Refering to figure 5, the non-linearity variation appears to be sharper at low speed, thus the controller grid is shosen finer below 5 m/s than above. The lateral operating range exibits a fairly regular shape, thus the grid is evenly distributed along this axis. Thus, the non-linear controller relies on twenty local models parametrized by two scheduling variables, the measured longitudinal velocity Vx and the yaw rate demand r_c. The figure 8 exibits the resulting non-linear gains $Kp(r_c, Vx)$ and $Ki(r_c, Vx)$.

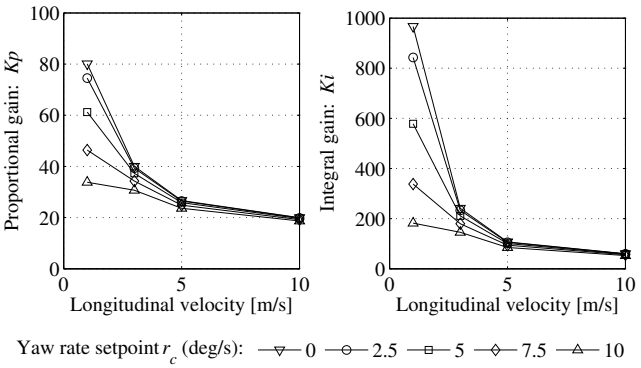

Fig. 8. Scheduled controller gains vs Vx and r_c

Finally, figure 9 outlines the global control structure for the automatic piloting configuration.

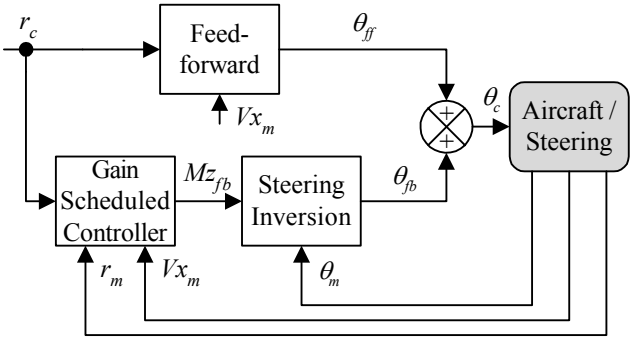

Fig. 9. Block diagram of the global controller

An anti windup action is applied to the controller integral term in order to cope with the angular rate saturation of the steering system. This term freezes the integral state when the maximum current is delivered to the steering servovalve.

4. ROBUSTNESS ASSESSMENT

The local stability of the controlled system has been studied by varying the uncertain parameters. The table 1 depicts the variation range of these parameters.The controller turns out to be very robust to parameters uncertainty. As figure 10 shows, the controller dynamics does not vary in a large scale and the smallest phase margin is over 60 deg. The open loop phase does not cross the -180 deg axis, it reveals that the system remains conditionally stable and has infinit gain margin. This local stability margin is widely sufficient to cope with the potential

Table 1. Parameters variation range

Parameter	Unit	Nominal value	Range
m	kg	$68 \cdot 10^3$	$[42\,;78] \cdot 10^3$
Lx_M/Lx_N	-	0.1	[0.05 ; 0.15]
C_M	rad^{-1}	3.78	[1.89 ; 7.56]
C_N	rad^{-1}	4.17	[2.09 ; 8.34]

vehicle dynamics variations. The system appears to be fairly under stressed, this is voluntary to cope with the saturation aspects that are not taken into account in the synthesis model. The global stability has been assessed from simulation results.

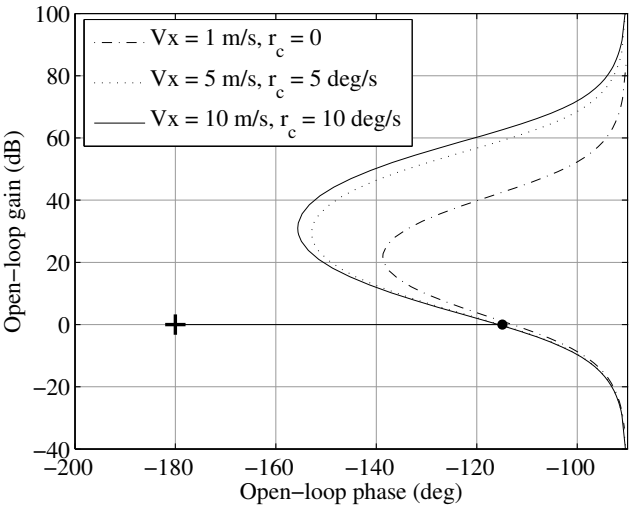

Fig. 10. Black chart of the open-loop controlled system

5. SIMULATION RESULTS

The control law has been validated on the complete 3-dimensions model. The figure 11 exhibits a two steps response of 4 deg/s at a longitudinal speed of 2 m/s with the heaviest aircraft on a dry surface. This simulation makes the controller operate at an interpolated point in between four models (Fig. 8).The propulsion is achieved by the wheel actuators but no differential driving is applied. The yaw rate response r_m reaches the reference r_c in an acceptable period of time with no steady state error and only a slight overshoot for the second step. The settling time is mostly driven by the steering rate saturation as the second subplot shows. Between 1 and 3.5 sec, and latter between 6 and 8.5 sec, the slew rate saturation of the steering system limits the response. The commanded angle θ_c reaches high magnitudes because of the combination of the feedforward term θ_{ff} and the controller action. Nevertheless, the latter additional command does not influence the system since the steering is already in saturation. Simulations performed at different speeds and several yaw rate demands give similar results.

6. CONCLUSION

The proposed yaw controller, based on local model pursuit and gain scheduling, achieves satisfactory performances on the entire operational range. The combination of feedforward tracking and local regulation gives comfortable robustness to parameter uncertainty. The reference adaptation makes the solution suitable for both manual driving and automatic piloting. The results, partially validated on a complete 16-D.O.F. model, must be evaluated by real ground tests. Additional MLG differential driving will be investigated to support the steering action and improve the overall yaw control performances and robustness.

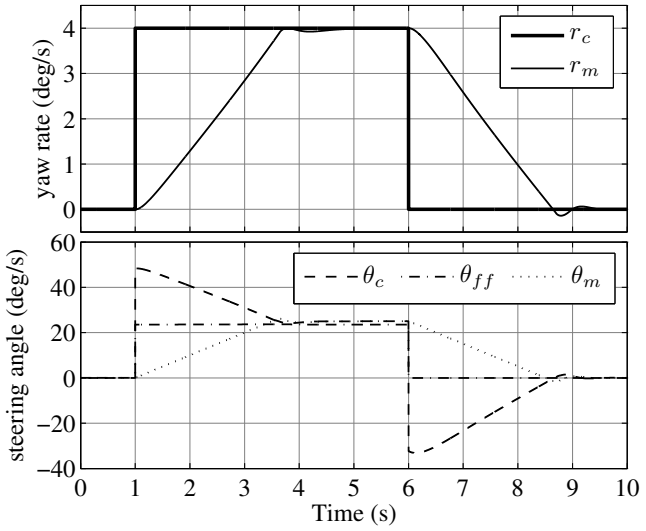

Fig. 11. Response to a step demand of 4 deg/s at a speed of 2 m/s

REFERENCES

Albero, F. (2009). Dymola A320 wheel model. Technical Report ESR00587-24, Messier-Bugatti.

Duprez, J., Mora-Camino, F., and Villaume, F. (2004). Aircraft-on-ground lateral control for low speed maneuvers. In *16th IFAC Symposium on Automatic Control in Aeropsace*. St. Petersburg, Russia.

Jacquet, A. (2008). *Nouveau concept de lois de commande intégrées pour un système de freinage d'avion*. Ph.D. thesis, Université de Haute Alsace.

Leithead, W. (1999). Survey of gain-scheduling analysis design. *International Journal of Control*, 73, 1001–1025.

Mauder, M. (2008). Robust tracking control of nonholonomic dynamic systems with application to the bi-steerable mobile robot. *Automatica*, 44, 2588–2592.

Pourboghrat, F. and Karlsson, M.P. (2002). Adaptive control of dynamic mobile robots with nonholonomic constraints. *Computers and Electrical Engineering*, 28, 241–253.

Roos, C. and Biannic, J.M. (2006). Aircraft-on-ground lateral control by an adaptive LFT-based anti-windup approach. In *IEEE Conference on Control Applications*, 2207–2212. Munich, Germany.

Rugh, W.J. and Shamma, J.S. (2000). Research on gain scheduling. *Automatica*, 36(10), 1401–1425. doi: 10.1016/S0005-1098(00)00058-3.

Slama, A. (2009). Dymola A320 aircraft model. Technical Report ESR00587-25, Messier-Bugatti.

Teo, A., Rajashekara, K., Hill, J., and Simmers, B. (2008). Examination of aircraft electric wheel drive taxiing concept. In *SAE Power Systems Conference*. Seattle, USA.

Villaume, F. (2002). *Contribution à la commande des systèmes complexes : application à l'automatisation du pilotage au sol des avions de transport*. Ph.D. thesis, Université de Toulouse III.

Zheng, B. and Anwar, S. (2009). Yaw stability control of a steer-by-wire equipped vehicle via active front wheel steering. *Mechatronics*, 19, 799–804.